energies

MDPI

Article

Methodology for the Detection and Classification of Power Quality Disturbances Using CWT and CNN

Eduardo Perez-Anaya [1], Arturo Yosimar Jaen-Cuellar [2], David Alejandro Elvira-Ortiz [2], Rene de Jesus Romero-Troncoso [1] and Juan Jose Saucedo-Dorantes [1,2,*]

[1] Engineering Faculty, Autonomous University of Queretaro, Campus San Juan del Río, Av. Río Moctezuma 249, San Juan del Rio 76807, QRO, Mexico; eperez87@alumnos.uaq.mx (E.P.-A.); troncoso@hspdigital.org (R.d.J.R.-T.)

[2] Academic Center of Advanced and Sustainable Technology (CATAS), Autonomous University of Queretaro, Tequisquiapan Campus, Carretera No. 120, San Juan del Río-Xilitla, Km 19+500, Tequisquiapan 76750, QRO, Mexico; ayjaen@hspdigital.org (A.Y.J.-C.); delvira@hspdigital.org (D.A.E.-O.)

* Correspondence: jsaucedo@hspdigital.org

Abstract: Energy generation through renewable processes has represented a suitable option for power supply; nevertheless, wind generators and photovoltaic systems can suddenly operate under undesired conditions, leading to power quality problems. In this regard, the development of condition-monitoring strategies applied to the detection of power quality disturbances becomes mandatory to ensure proper working conditions of electrical machinery. Therefore, in this work we propose a diagnosis methodology for detecting power quality disturbances by means of the continuous wavelet transform (CWT) and convolutional neural network (CNN). The novelty of this work lies in the image processing that allows us to precisely highlight the discriminant patterns through spectrograms into 2D images; the images are cropped and reduced to a standard size of 128x128 pixels to retain the most relevant information. Subsequently, the identification of six power quality disturbances is automatically performed by a convolutional neural network. The effectiveness of the proposed method is validated under a set of synthetic data as well as a real data set; the obtained results make the proposal suitable for being incorporated into the monitoring of power quality disturbances in renewable energy systems.

Keywords: power quality disturbance; condition monitoring; continuous wavelet transform; convolutional neural network

Citation: Perez-Anaya, E.; Jaen-Cuellar, A.Y.; Elvira-Ortiz, D.A.; Romero-Troncoso, R.d.J.; Saucedo-Dorantes, J.J. Methodology for the Detection and Classification of Power Quality Disturbances Using CWT and CNN. *Energies* **2024**, *17*, 852. https://doi.org/10.3390/en17040852

Academic Editor: Dinko Vukadinović

Received: 28 December 2023
Revised: 7 February 2024
Accepted: 9 February 2024
Published: 11 February 2024

1. Introduction

Nowadays, electric power generation has taken a turn towards the implementation of renewable energies (RE), a situation that supposes not only a change but a challenge. Therefore, the power system is suffering a transition that is being carried out in a gradual and controlled manner. The International Renewable Energy Agency (IRENA) estimates that by 2050, around 90% of the power demand around the world can and should come from renewable energies [1] Currently, power generation systems are based on the burning of fossil and mineral fuels, but this way of production is facing environmental and economic problems, becoming less and less profitable every day. Thus, many global policies are encouraging the implementation of distributed generation systems that include renewable sources. This way, we can achieve greater sustainability because the use of RE reduces the amount of green-house gas emissions, which are related to air pollution and climate change. However, RE are susceptible to problems related to power quality (PQ), which is derived from the erratic behavior of renewable generation systems [2]. In this sense, some conditions like the shadows generated by clouds and buildings [3,4], the accumulation of dust, snow, or dirt generated by wildlife [5,6], and the temperature [7], all impact the performance of the photovoltaic system (PVS) by obstructing the solar radiation that reaches

the system, decreasing its performance by up to 20%, as shown in [8]. All these variations downgrade the amount of generated power, but they also degrade the PQ [9]. This is not a minor situation, because when the PVS is interconnected to the grid, the disturbances related to the use of RE are also incorporated into the conventional grid, affecting the end-users. Therefore, PQ has become a topic of interest because it has been shown to have an impact on the performance of both electrical and electronic equipment. The term PQ derives from a standard given by IEEE std 1159 [10], which specifies the ideal characteristics that the sinusoidal signal should have both in frequency and magnitude to ensure optimum operation of the equipment. Within this same standard, certain anomalous behaviors are already defined and called power quality disturbances (PQD). Some of the most common can be classified as sag, swell, fluctuations, harmonics, and transient impulses. Additionally, each of these disturbances has its own well-defined characteristics that serve as a basis for the detection, classification, and mitigation of these types of disturbances when they appear in an electrical signal.

Due to the importance of PQ, a number of processing tools and techniques have been developed to address the presence of disturbances and anomalies in power systems. The events related to PQ may be classified as stationary and non-stationary depending on the nature of the phenomenon [11], and they have different behaviors in time, frequency, and amplitude. Therefore, the developed processing techniques must be able to properly identify variations and deviations in all these magnitudes. Several signal processing techniques have been used to address this problem; some of them use frequency analysis by means of the Fourier transform (FT) [12]. Although this technique provides good results, it is limited because it does not provide temporal information and is focused only on the analysis of stationary signals. Additionally, some other more specialized techniques have been used to perform not only a frequency track, but also a time-frequency analysis, such as the wavelet transform (WT) [13], empirical mode decomposition (EMD) [14], the short time Fourier transform (STFT), the S-Transform (ST), continuous wavelet transform (CWT) [15], and the Hilbert Huang transform (HHT) [16], among others. Due to their ability to perform an adaptive time and frequency trace, these methods are suitable for analyzing transient, nonlinear and non-stationary signals, and they have shown good results in the analysis of PQD. Each of these techniques has characteristics that improve or decrease its performance depending on the analyzed signal. The CWT, for example, is one of the most used techniques due to its windowing characteristic that allows precise monitoring in frequency, time, and magnitude resolution, providing versatility and adaptability to treat a vast number of signals within different frequency ranges. Recently, these time–frequency techniques have been considered from an image processing point of view because the resulting spectrogram is in fact an image, and spectral component information may be extracted from it. For instance, in [17], the STFT and the S-Transform are used to obtain different spectrograms that help to characterize different PQD, such as voltage sag, voltage swell, momentary interruption, harmonic content, and DC offset. With the methodology proposed in that work, it is possible to visualize and classify these disturbances in an easy way, and it is demonstrated that the S-transform helps to improve the results delivered by the STFT. In a similar approach, the work in [18] uses the Chirplet transform (CT) and different time-frequency-scale transform (TFST) to show how it is possible to detect and classify different PQD through a spectrogram, facilitating the interpretation of the results. Even though these techniques have been shown to be useful in the detection of PQD, they still depend on the interpretation of the information by an expert user, whether performing a direct parameter comparison based on statistical indicators or by visual comparison. This implies a drawback, because there is the possibility of misinterpretation, resulting in false positive or false negative situations that may cause permanent damage to the equipment connected to the grid. Additionally, it is important to mention that the amount of data obtained from the time-frequency domain techniques and the spectrogram images is huge, complicating the correct analysis of the results even more.

In order to improve the results delivered by the space-transform-based methodologies and to avoid the misinterpretations resulting from human error, some other methodologies have been developed to receive the large amount of data delivered from the analysis of the power signals and to perform automatic detection of PQD. In this sense, the methodologies that make use of deep learning (DL) and machine learning (ML) have gained popularity in recent years. These approaches are provided with the ability to learn; thus, they can be adapted to perform continuous monitoring that allows the automatic classification of different disturbances related to PQ. On the machine learning side, the work developed in [19] proposes an approach based on dimensionality reduction through a linear discriminant analysis (LDA); moreover, statistical features are used to characterize the behavior of different PQD, and finally, using a Neural Network as a classifier, it is possible to perform an automatic classification of the disturbance in the signal. Another example of this approach is presented in the work of [20]. Here, four main steps are defined: generation of PQD classes, feature extraction, selection of highly discriminating features, and then the classification of PQDs using selected features. Both approaches demonstrated high classification rates related to PQDs. On the other hand, the work presented in [21] analyzes different machine learning approaches that have been carried out in recent years. In that work, the authors show different techniques, like the support vector machine (SVM), artificial neural network (ANN), k-nearest neighbors (kNN), and fuzzy logic (FL). They test the effectiveness of all of them in the detection and classification of different PQD, demonstrating that machine learning is a suitable tool for this task. On the deep learning side, several works have been developed. For instance, in [22,23] the authors use an auto-encoder neural network to find the most representative features of PQ-related events in an automated way. Also, in [24] the large number of images and information required for the correct training of the network takes at least 87 min; thus, it requires a high computational effort and hinders its application in continuous monitoring systems. Moreover, they do not explore if image pre-conditioning (like resizing and zones cutting) may reduce the computational burden, preserving the accuracy of the methodology; finally, they only perform tests in synthetic signals, and it is not shown how the method responds to real signals. Even with the difficulties that may arise, there are works that have demonstrated that CNN is a powerful tool for the identification of deviations in electric signals. For instance, in [25,26] the authors applied the CNN for analyzing electrical motor failures using spectrogram images that show the benefits of working under a deep-learning scheme. Given the results obtained in different fields, it is possible that similar results can be obtained in the PQ field. One of the limitations of the discussed works is that most of them only work with ideal synthetic signals without the effects of noise contamination, achieving classification accuracies up to 97%, which do not reflect their performance under real conditions.

This work proposes a methodology for the automatic detection and classification of PQD using CWT and CNN as main tools. This approach is based on image processing techniques and pattern recognition. Therefore, a 2D image bank is generated from the spectrograms of different disturbances obtained by means of the CWT. To ensure that only the most relevant information is retained in the images, they are cropped, reducing their resolution by resizing the images to a standard 128 $\times$ 128 pixels. This way, the amount of data is highly reduced, and an improvement is achieved in the classification process that turns to the next task. Such classification is performed by a CNN that receives the resized spectrogram images as inputs and delivers the PQD that exists in the signal as outputs. The proposed methodology is validated first using synthetic signals that simulate six different PQ conditions: healthy signal, sag, swell, harmonic distortion, voltage fluctuation, and impulsive transient. Additionally, with the aim to improve the methodology strength by giving a synthetic signal with a level of realistic behavior, each one of the synthetic disturbances considered adding four levels of white Gaussian noise (0, 10, 20 and 30 dB). These signals are used to train the deep learning model and determine whether the methodology is suitable for performing the automatic classification of the PQD. Next, the proposed approach is tested with real signals coming from a 30 MW photovoltaic

park located in Spain. Since in this type of system it is necessary to guarantee that the voltage signal remains within very specific ranges in amplitude and phase, the proposed methodology considers the voltage signals from the PV system as the inputs to be analyzed. The novelty of this work consists of the use of real signals from a PVS and a preprocessing stage consisting of the reduction of the data set by applying a resize to the spectrogram images and using signals of short duration (maximum one minute). The obtained results show that the developed method can detect and classify a wide variety of PQD, making it a useful tool to assess the impact that a PVS may cause regarding PQ.

2. Theoretical Background

This section describes the theoretical aspects that are considered for performing the proposed diagnosis approach, relevant definitions of power quality disturbances (PQD) are given, and the general description of a CNN structure is mentioned.

2.1. Power Quality Disturbances

PQ is a general term that refers to a phenomenon that can affect electrical equipment when the power supply presents instabilities or disturbances associated with amplitude, continuity, waveform, and frequency. Therefore, the PQ is often measured through different international standards where the most important are the IEC 61000, IEEE 1159, and the EN 50160 [27,28]. Although different standards can be used to describe PQD, the IEEE 1159 is the most recognized one, and it is recommended and implemented for monitoring PQ; thus, five main disturbances such as sags, swells, transients, fluctuations, and harmonics are defined by the IEEE 1159 [10].

Therefore, three of these five disturbances are directly related to the amplitude of the voltage signal, and the other two are associated with changes in the frequency. Certainly, the sag is represented as a phenomenon that shows a loss of amplitude. The occurrence of sag can also be measured in terms of the RMS value of the voltage signal within a range from 0.1 to 0.9 pu (per unit) with a duration greater than 5 cycles in 60 s. On the other hand, the swell occurs when the voltage signal is subjected to amplitude increases of around 1.1 pu in terms of the RMS value and with a duration greater than 30 to 60 s. Although the sag and swell modify the amplitude of the voltage signal, the transient impulse appears as a sudden change in steady-state frequency conditions that can produce changes on both signals, voltage, or current, and is unidirectional in polarity; hence, this kind of disturbance is measured by quantifying the amplitude of the disturbance, the onset time, and the duration.

Regarding the disturbances linked to changes in the frequency, the harmonic distortion is known as the result from the sum of multiple frequencies of the fundamental component at which the system is intended to operate; consequently, the occurrence of harmonics leads to a waveform distortion, and it can be evaluated by estimating the total harmonic distortion (THD). According to the standards, the THD level must be lower than 8% in power grids that operate under voltages lower than 1.0 kV. Finally, voltage fluctuations are conditions where random changes in the voltage signal appear. Such changes can also be defined as systematic variations of the signal envelope within ranges from 0.95 to 1.05 pu.

2.2. Continuous Wavelet Transform (CWT)

Condition monitoring strategies are commonly supported by signal processing techniques that allow highlighting those fault-related patterns; hence, the time domain, frequency domain, and time–frequency domain remain the most preferred processing techniques, and each one of them can be selected according to specific aims. Certainly, time–domain processing techniques represent a practical solution, since trends and changes of the signals can be modeled through the estimation of statistical features with an excellent trade-off between simplicity and performance [29]. By their part, frequency domain techniques represent some of the most reliable approaches since the existence of specific undesired frequency components on the signal usually indicates malfunctioning problems [30]. On

the other hand, time-frequency techniques are also incorporated for the processing of signals due to their capability of providing temporal and spectral information.

In this sense, the continuous wavelet transform (CWT) is considered a time–frequency technique that allows the analysis of multiscale non-stationary signals using a windowing approach to extract information from segments of a signal [31]. These signal segments are then evaluated by a window called mother wavelet [32], this process allows the CWT to have the versatility of lengthening or shortening the window size depending on the selected scale of the mother wavelet. Consequently, a smaller scale is associated with a greater sensitivity in frequency variations; Equation (1) depicts the mathematical expression:

$$C(a,\ \tau) = \int \frac{1}{\sqrt{a}} \psi\left(\frac{t-\tau}{a}\right) x(t)dt \tag{1}$$

where C is the transform, a is the scale factor, τ is the overlap time, ψ is the mother wavelet function, and $x(t)$ is the signal input as a function of time.

Hence, one of the main advantages of the CWT is its capability of contraction and dilation, which can lead to high spectral resolution depending on the needs of the signal to be analyzed. Likewise, an additional property of the wavelet function is that it can obey a certain limit, since the energy represented must be finite and must meet the admissibility condition. These parameters are described by Equations (2) and (3), respectively.

$$E = \int_{-\infty}^{\infty} |\psi(t)|^2 dt \tag{2}$$

$$E = \int_{-\infty}^{\infty} \psi(t)dt = 0 \tag{3}$$

where E is the energy of the wavelet and ψ is the wavelet mother function.

The graphical representation of the correlation between the waveform scale and time is known as a Scalogram; subsequently, the CWT automatically adjusts the time and frequency based on the resolution, depending on the contraction or dilation of the window that best fits the signal to be analyzed [33]. Within this same aspect, there is another representation offered by the CWT, which shows a time-frequency-scale distribution mapping the distribution of the energy contained within the signal expressing this energy per unit frequency. This representation is known as the spectrogram [34]. This last feature makes the CWT suitable for the analysis of non-stationary signals since this representation considers the three main characteristics that make up a signal, showing them graphically, and facilitating their interpretation.

2.3. Convolutional Neural Network

Convolutional neural networks (CNN) have been widely used in several methods based on image classification under large sets of information; certainly, a CNN is a feed-forward network that uses partial variance to learn behavioral patterns, and it is specifically designed for image processing [34]. As in any network structure, the input layer of the CNN evaluates the set of original images to be processed, obtaining an output block that contains the estimated features derived from the original image. Accordingly, a series of filters are applied for further processing. These filters consist of four main processes, where the first one consists of a convolutional layer, polishing, vectorization, and classification. These are described in more detail below.

Convolutional layer: A convolutional layer is the main component in a CNN containing a series of filters (Kernels), which map the image by generating a new space through convolutions [35]. This means that from the original image, the most representative features are extracted as the filtering process progresses. Equation (4) shows the process carried out by a convolutional network.

$$y_j^k = \sum W_{ij}^k * x_j^k + b_j^k \tag{4}$$

where y_j^k is the mapping feature output, x_j^k is the plane feature input, W_{ij}^k is the 2D filter set, and b_j^k is the bias training parameter.

Polishing layer: The polishing layer is a non-linear process that reduces the sample size. This process is performed to reduce the number of patterns that will be fed to the training process without losing a large amount of information in the process. This feature extraction process when performing max-pooling is given by Equation (5).

$$h_r = max_1^{MxM}(X_{pj}) \tag{5}$$

where h_r is the output of the features when mapping, X_{pj} is the element of the clustered region, and M is the size of the clustered mapping dimension.

Flattened layer: This layer is responsible for applying a vectorization process of the mapping performed by the previous layers, forming a vector that contains the information already processed by the whole stages of convolution and polishing, generating a concentrated vector of features that can be more easily processed by the classification layer.

Classification layer: The classification layer oversees processing all the information delivered by the vectorization layer when performing a class classification process employing activation functions. One of the most used for the solution of class classification problems is the "Softmax" [36]. Image processing through CNN is a highly recommended and widely used procedure to tackle different classification and pattern detection problems, some related works can be found in references [35,37].

3. Proposed Methodology

The proposed methodology for detecting and classifying PQ disturbances occurring in photovoltaic cogeneration systems is presented through the general block diagram of Figure 1. As can be noticed, three main stages encompass the methodology to know: (i) Signals bank, (ii) Image processing, and (iii) Pattern recognition and classification.

First, a description of the stage "Signals banks" is presented. Here, two different sets of signal banks (voltage signals) are used for processing by the proposed methodology; on one hand, there is the bank of synthetic signals, and on the other hand, there is the bank of real signals. The set of synthetic voltage signals are generated having a fundamental frequency of 60 Hz with a sampling rate of 8 kHz during 0.3 s. Therefore, these signals presented in Figure 2. comprise the healthy state (ideal sine wave behavior) and five different types of power quality disturbances, such as sag (SAG), swell (SWL), flicker (FLC), harmonic content (HAR), and transient impulse (IMP). Additionally, with the purpose of being considered as power disturbances, their generation considered the normativity established by the standard IEEE-1159 in relation to parameters like duration, amplitude, and frequency [10]. Now, assuming that a synthetic signal behaves somewhat ideally and cannot provide enough variability, some noise is added to test the strength of the methodology. As a consequence, white Gaussian noise is added to the synthetic signal, and this is repeated in four different noise levels (0 SNR dB, 10 SNR dB, 20 SNR dB, and 30 SNR dB), generating 250 images per level, leaving a total of 1000 images per synthetic signal. By its part, the bank of real signals comprises a signal from a photovoltaic cogeneration system in Spain, located in the south-central area of the country, which is a 30 MW photovoltaic power plant. The acquisition of the signal was performed on a 100 kW three-phase inverter at 230 RMS volts with a fundamental frequency of 50 Hz with sag disturbances. In Figure 3, an example of the acquired signal under the occurrence of SAG is shown. It must be emphasized that signal acquisition should always be performed as close as possible to the point of interest for the analysis since this ensures measurements without environmental or structural interferences that may affect the data collection. In this specific case, the subjects of interest were the PQ signals generated by the cogeneration system, so the acquisition was performed as close as possible to it in one of the phases of the inverter. The amplitudes of all the signals are normalized, and the units remain as *per-units* (pu).

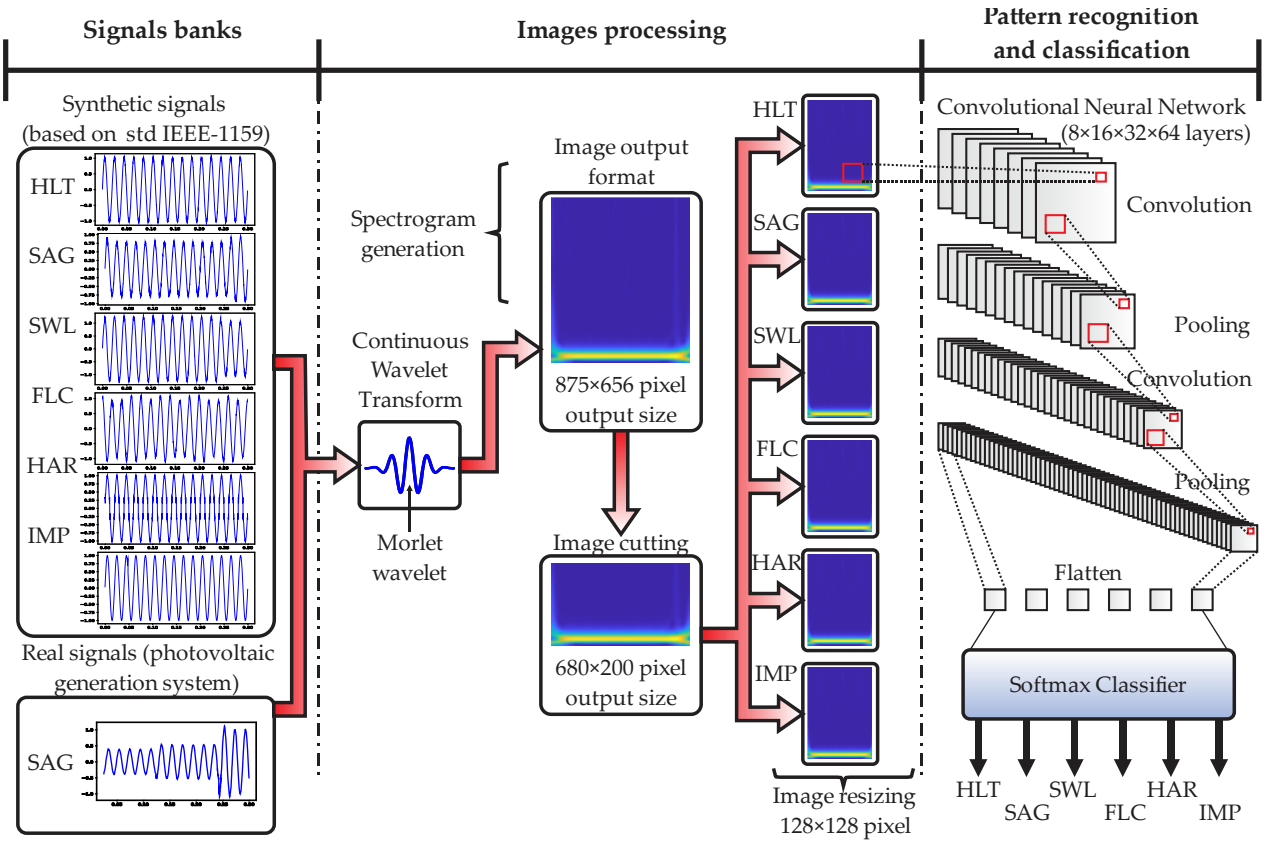

Figure 1. General block diagram of the proposed methodology based on CWT and CNN for detecting and classifying standardized PQ disturbances.

In the second stage of the proposed methodology "Images processing", the synthetic signals coming from the first bank are processed through the continuous wavelet transform (CWT). To perform the CWT, the analytic Morlet-Gabor is selected as the mother wavelet, and an extended signal configuration is used to mitigate the boundary effects. This way, the normalized voltage signals are transformed into 2D images, having the information about whether a power disturbance appears or not. Thus, through the CWT, a spectrogram image is generated from the original signal as output with an original format of 875 × 656 pixels. However, since not all the zones of the image contain relevant information about the power disturbance, it is necessary to cut the upper area of the spectrogram, leaving only the bottom area where the magnitude components are observed, yielding a clipped frame of 600 × 200 pixels size. Additionally, with the aim of reducing the computational effort required to process the data, a resizing is performed to this new frame, yielding a final image with a format of 128 × 128 pixels. This procedure will be repeated for each one of the six signals (normal signal and the five signals with power disturbances), considering the free noise (250 samples) signal and the three noise levels per disturbance condition (750 spectrograms); then, a total of 6000 resized spectrograms are finally generated.

The third stage, named "Pattern recognition and classification", consists of applying a classifier structure based on deep learning, which in this case is a convolutional neural network (CNN) ideal for processing data in image format. This way, the final images of 128 × 128 pixels with the different noise levels are fed into the network with a binary structure that considers four hidden convolutional layers of 8, 16, 32, and 64 neurons, respectively. The vectorized output from the CNN (flatten layer) is finally processed by a SoftMax multiclass classifier with the purpose of labeling the type of power disturbance contained in the spectrogram. The training process of the CNN considers Stochastic Gradient Descent Momentum (SGDM), and the convolution layers have a Rectified Linear Unit (ReLU) activation function. With this, the network training speed is increased, and

the convergence of the gradient descent algorithm is ensured. What exactly happens is that the CNN learns patterns about the power disturbances contained in the spectrogram image, and then SoftMax provides a final label of the specific disturbance found. It is worth mentioning that the images are first fed to the CNN for training purposes, but some images are reserved for validation, and additionally, some images from the real data bank are tested to probe the methodology effectiveness. The detailed description of the network structure, and the percentage of data considered for training and validation, are also specified in the next section.

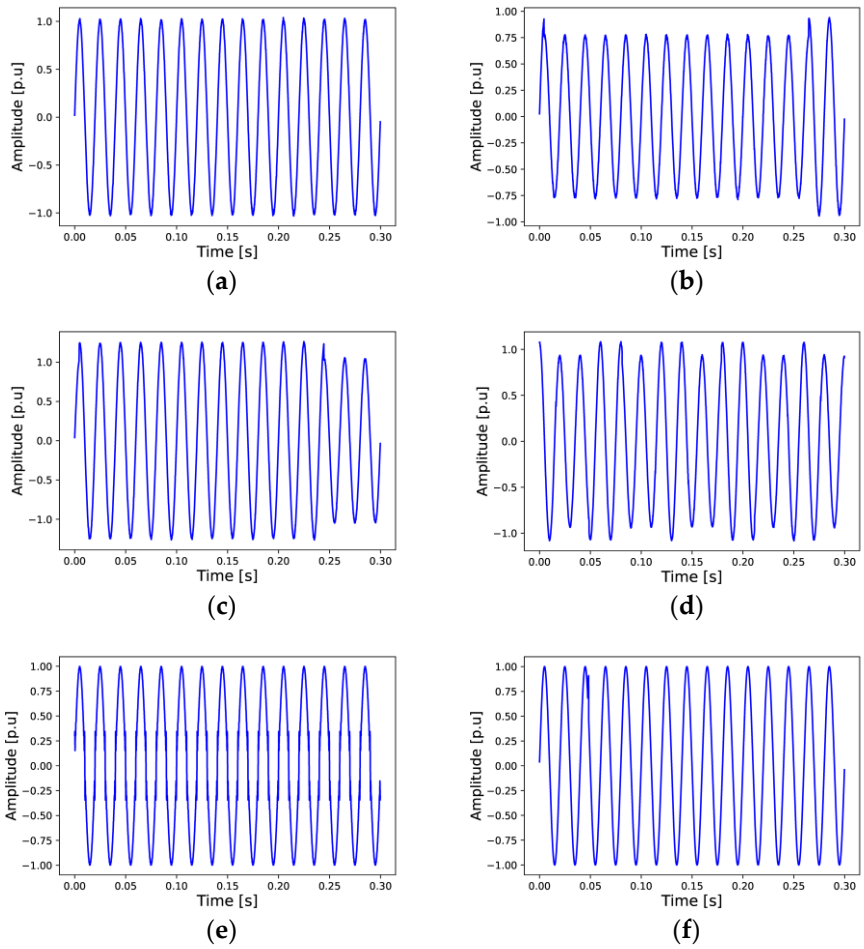

Figure 2. Synthetic signals considered for the evaluation of the proposed methodology; each one of the signals represents: (**a**) healthy condition (HLT), (**b**) voltage sag (SAG), (**c**) voltage swell (SWL), (**d**) flicker (FLC), (**e**) harmonic content (HAR), and (**f**) transient impulse (IMP).

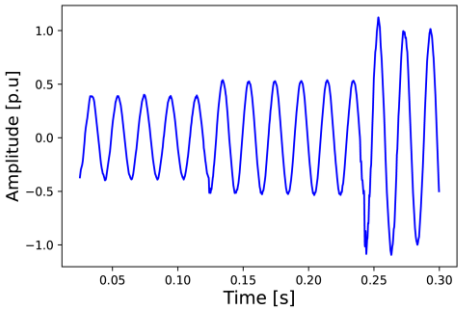

Figure 3. Real signal acquired from a photovoltaic cogeneration system with sag disturbance.

4. Results

This section is divided into two main parts. The first one presents the results that are achieved when the proposed diagnosis methodology is applied to a bank of synthetic signals, and the second one shows that the results that are carried out when real signals from a 30 MW PVS located in Spain are evaluated through the proposed approach.

4.1. Competency of the Proposed Methodology in Front of Synthetic Signals

The proposed methodology is first evaluated under a bank of synthetic signals in order to validate its applicability to real systems. Thus, as mentioned previously, a bank of synthetic signals is generated involving a total of six different conditions: healthy signal (HLT), voltage sag (SAG), voltage swell (SWL), harmonic distortion (HAR), voltage fluctuations (FLC), and impulsive transient (IMP). Such synthetic signals are generated by considering the mathematical formulation presented in [38], thereby, for each one of the considered conditions, a total of 1000 signals with a duration of 0.3 s are synthetically generated. Indeed, it should be mentioned that these signals were randomly generated, but the duration, location, and severity are within the parameters established by the standard IEEE 1159. Moreover, white Gaussian noise has been added to the generated signals to ensure their similarity to those that appear in real conditions; hence, the noise was added by considering random SNR values from 0 dB to 40 dB. Accordingly, the synthetic signals were generated as shown in Figure 2, where it is possible to appreciate the waveform of the conditions under study, such as for the healthy condition, voltage sag, voltage swell, flicker, harmonics, and transients, respectively.

In addition, it can be observed from the synthetic signals of Figure 2 that the amplitude of each one of them is expressed as per unit (p.u.) as is defined in the standard IEEE 1159. Certainly, the use of p.u. is a mandatory suggestion that must be followed during the implementation of monitoring strategies since this particular scale defines the amplitude parameters of any PQD. Consequently, the implementation of the proposed methodology to real signals may consider a normalization process in order to ensure the proper assessment and identification of disturbances. Additionally, it is observed that the disturbances are present in the signals, but its identification usually requires expertise; on the other hand, it is common to make mistakes during the identification of PQD when the assessment is carried out by visual inspection. This assertion is due to how there are some disturbances that are difficult to detect even by experts. For instance, the IMP disturbance in Figure 2f presents a low amplitude and a short duration, making it difficult to find. Therefore, the development of an efficient strategy to identify and classify the PQD remains necessary.

Thus, following the proposed methodology, the synthetic signals are then subjected to a processing stage by means of the CWT; as a result, a spectrogram represented by a 2D image is obtained for each one of the signals. Consequently, a set of 1000 images is generated for each condition under study; afterward, the images are preprocessed with the aim of reducing the amount of data that must be treated without compromising the information provided by the image. Such preprocessing is mainly performed for resizing the original images as shown in Figure 4; thereby, all the images are scaled to a new size by preserving the most important information.

The 2D spectrogram presented in Figure 4 belongs to one of the generated signals that simulate a voltage sag. The spectrogram is obtained by applying the DWT to the signal under evaluation, and then it is saved as an image with an original size of 875 $\times$ 656 pixels. It is observed that the original image provides relevant information regarding the disturbance behavior; for instance, a frequency component linked to the fundamental frequency appears horizontally in yellow at the bottom of the image, but at the beginning and at the end of the 2D spectrogram, it can be noticed that there are changes that affect the amplitude of the fundamental component. These amplitude changes are due to the occurrence of the voltage sag, and this is explained because the signal being analyzed is healthy at the beginning, but around 0.02 s, the voltage sag starts; then, the voltage sag remains until 0.25 s, when the healthy condition returns. It should also be highlighted that

during the transition from sag to healthy condition, a faint line appears that is relevant for the identification of amplitude variations. In this regard, a first size reduction is carried out by making a crop to the original image with the aim of removing most of the redundant information, but the most relevant information is preserved. The region of high frequencies is completely removed from the original 2D spectrogram by applying the cropping, thus, although it could be thought that relevant information is being eliminated, it should be mentioned that high frequencies do not provide significant information from the viewpoint of power quality analysis. Finally, the image is resized to a standard 128 × 128 pixel size; hence, despite the size reduction to 128 × 128 pixels, it is still possible to observe the amplitude changes at the beginning and at the end of the signal. Truthfully, the faint line that depicts the transition from the disturbance to the healthy state remains in the final image, proving that the relevant information is preserved after the resizing. Although the processing that is applied to the images seems trivial, it has a significant impact, since it allows us to significantly reduce the amount of data processed by the CNN; consequently, the computational burden is also reduced.

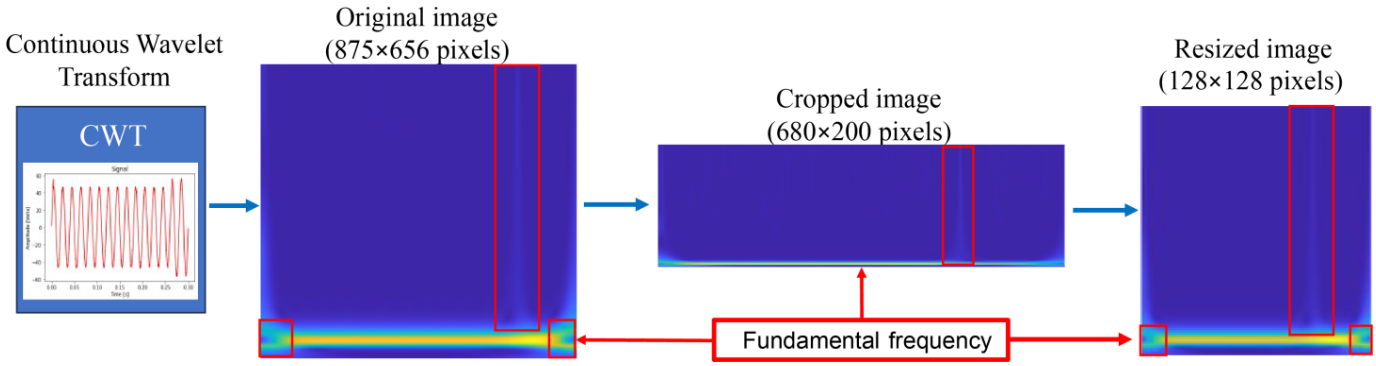

Figure 4. Resizing process to reduce the amount of data without losing information.

Hence, the resizing procedure is applied to all images of all considered conditions; then, the new images are used as input in the CNN structure in order to carry out the classification task. Due to there being a total of 6000 spectrograms (1000 per disturbance) that compose the dataset under assessment, 60% of the 2D spectrograms is used during the training process, 20% is used for testing purposes, and the remaining 20% is used for validation. Afterward, the CNN structure is subjected to the training procedure for 550 iterations, leading to achieving an accuracy of around 99.41% during the test process and a maximum value of around 99.48% during the validation. In Figure 5, the qualitative representation of the accuracy that was reached during the training of the CNN is shown. The achieved accuracy is promising, and it can be considered as a metric that validates the effectiveness of the proposed methodology and its feasibility for being applied in the detection and classification of PQD. On the other hand, Figure 6 shows the qualitative representation of loss achieved by the CNN, which at the end of the process tends to zero. From the results presented in Figure 6, it can be inferred that the hyperparameters of the CNN are well-adjusted, and therefore, it is expected that the classification errors remain low. Regarding the individual classification for each one of the assessed conditions, the confusion matrix obtained during the individual classification is presented in Table 1. As observed, for the HLT, FLC, HAR, and IMP conditions, 100% of the individual classification is achieved, whereas the SAG and SWL conditions reached an individual classification of about 99.0% and 97.5%, respectively. Only two and five misclassification errors were made between the SAG, SWL, and the HLT conditions. Although the proposed classifier sometimes produces classification errors and confuses the SAG and SWL conditions with the HLT one, this is an expected situation, because all the generated signals have at least a part of the HLT condition. Nevertheless, the high-performance of the accuracy indicates that the proposed methodology has the capability to detect and classify different disturbances, and it can be used as a diagnostic tool for assessing the quality of power grids.

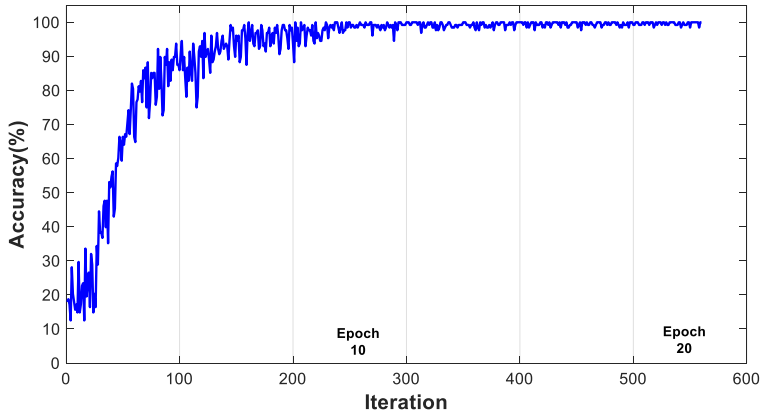

Figure 5. Qualitative representation of the accuracy achieved by the CNN structure during the training procedure.

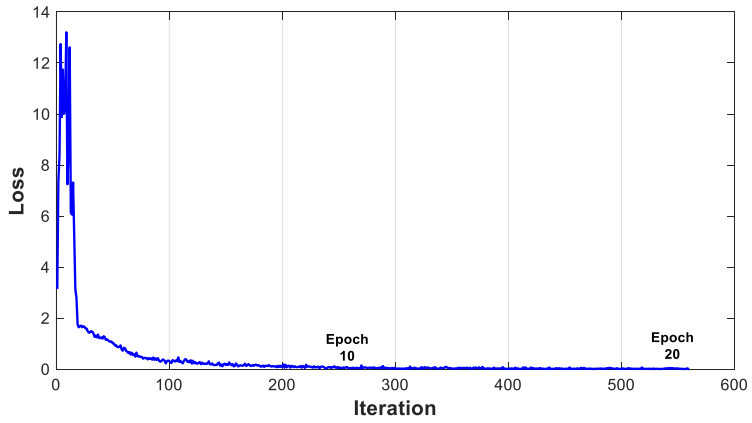

Figure 6. Qualitative representation of the loss achieved by the CNN structure during the training.

Table 1. Confusion matrix achieved by the CNN structure during the validation for all assessed conditions.

		True Class					
		HLT	**SAG**	**SWL**	**FLC**	**HAR**	**IMP**
Assigned Class	HLT	200	2	5	0	0	0
	SAG	0	198	0	0	0	0
	SWL	0	0	195	0	0	0
	FLC	0	0	0	200	0	0
	HAR	0	0	0	0	200	0
	IMP	0	0	0	0	0	200

Finally, for practical implementation, it should be mentioned that the proposed methodology has been implemented in a personal computer with an intel core i7-12700H 12th gen (4.7 GHz), and the image processing is configured to be performed by a dedicated GPU NVIDIA GeForce RTX 3070 (Manufactured by Micro-Star International-MSI Co., Ltd., New Taipei City, Taiwan). In this sense, the whole process is carried out in an approximated time of 120 s, which is a relatively short time of response considering that the processing is purely carried out on images.

4.2. Study Case: 30 MW Photovoltaic System

Once the proposed method is successfully applied to identify and classify different PQD through the analysis of synthetic signals, the analysis of real signals acquired from a real electric system is then carried out. Certainly, the experimentation is performed with

the voltage signals acquired from a PV generation plant located in south-central Spain; such PVS can generate a total of 30 MW, and it is interconnected to the local grid. The measurement of electric signals is carried out in a 100 kW three-phase PV inverter with a nominal voltage of 230 Vrms at 50 Hz. The acquired signals are measured in this place because it has been demonstrated that the PQD that appear in a power grid are produced due to the action of the loads that are connected to grid; therefore, the measurement is performed in the AC side of the PV inverter, which is the device in charge of feeding the loads connected to the grid. Hence, it is important to mention that current signals in a PV system can present many natural variations throughout the day. These variations occur because the current delivered by the PV system is determined by the amount of solar radiation that reaches the PV panels. In this sense, the current signals are not suitable to be analyzed, but the voltage signals must always remain at an amplitude of 230 Vrms with a 50 Hz frequency; therefore, any deviation from these values may be dangerous for the equipment connected to the grid. Accordingly, the analysis of PQD through the analysis over voltage signals is adequate.

Consequently, the signals are acquired and stored using a proprietary data acquisition system (DAS) based on field programmable gate array (FPGA) technology; the DAS is able to acquire the three-phase voltages and currents at the same time at a sampling frequency of 8000 Hz. Although the PVS is designed to keep the failures and disturbances to a minimum, it eventually presents some undesired phenomena. As mentioned before, the real signals are subjected to a normalization procedure in order to transform the original amplitudes into the p.u. scale. Afterward, the proposed methodology is applied as described in Section 3 in order to carry out the assessment and identification of PQD. In this sense, Figure 7a shows a voltage sag that was identified by the proposed methodology; as observed, the occurrence of two different severities of voltage sag produces effects in the voltage signal during 3 s. Thus, two main different amplitudes are identified. The first one is around 0.4 p.u., and the second one is about 0.6 p.u. Finally, at around the 0.25 s, the signal returns to a normal amplitude that falls within the permitted range established by the standard IEEE 1159. Additionally, the corresponding 2D spectrogram obtained by the CWT is shown in Figure 7b, where it can be seen that there are two faint lines that represent the two changes in the amplitude of the signal. However, the fundamental component of frequency cannot be clearly appreciated in Figure 7b since it is hindered by the background noise. In this sense, the image resizing procedure is then applied as a filter that allows highlighting the fundamental frequency component due to non-useful frequencies (high-frequencies) being removed from the original spectrogram (see Figure 7c)). Also, it is observed that the two lines that depict the amplitude changes of the signal are more visible in the resized image than in the original one, marking the importance of the resizing process in this methodology being able to achieve accurate results while reducing the computational burden.

The proposed methodology also has the capability to detect other different PQD; hence, an impulsive transient is also identified in the 30 MW PVS as presented in Figure 8a. In fact, it is necessary to zoom in over the affected signal zone in order to clearly identify the appearance of the impulsive transient; hence, it must be highlighted that the identification of this kind of disturbance is difficult through a visual inspection. Then, the CWT is applied over the affected signal to obtain its corresponding 2D spectrogram (see Figure 8b), and a line appears extended over the entire range of frequencies. This line is located around 0.1 s, approximately. Afterward, the resizing procedure is carried out, highlighting the details of the 2D spectrogram (see Figure 8c). The final 2D spectrogram may facilitate the identification and classification of the disturbance performed by the CNN.

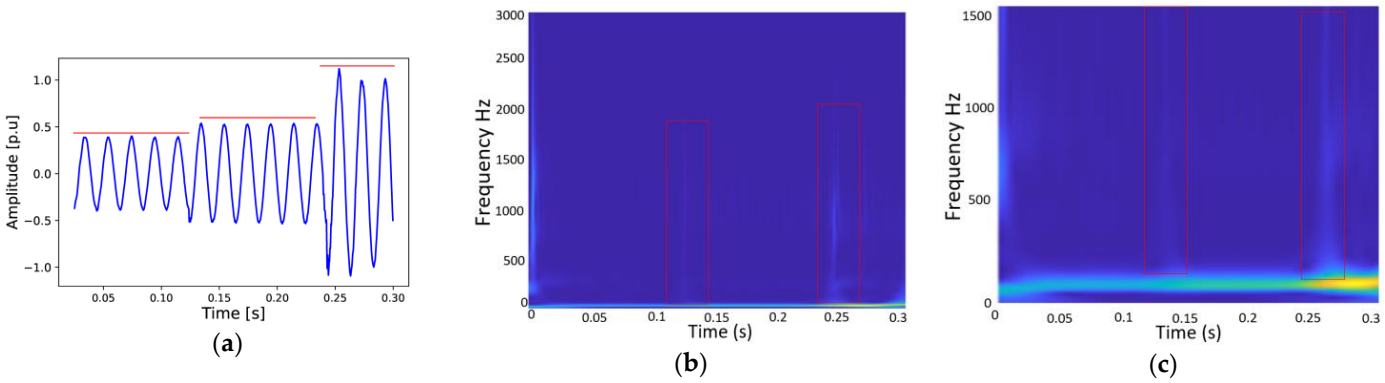

Figure 7. Real signal acquired from the 30 MW photovoltaic system, (**a**) voltage signal under the occurrence of SAG (horizontal red lines represent different SAG severities), (**b**) its original 2D spectrogram obtained by means of the CWT and, (**c**) the resized 2D spectrogram obtained after the resizing procedure.

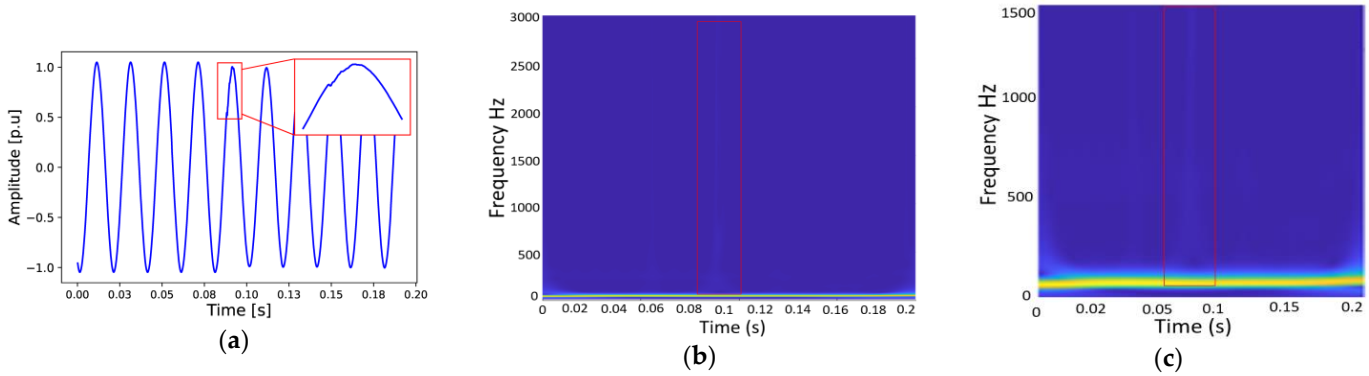

Figure 8. (**a**) real signal from the PVS with an impulsive transient (red rectangle), (**b**) original spectrogram image obtained by means of the CWT over the signal with the impulsive transient (red rectangle indicates the occurrence of impulsive transient), and (**c**) resized spectrogram of the signal with impulsive transient.

It is worth mentioning that there are some other methodologies that do not require the use of images. Such methodologies use a waveform approach by analyzing the amplitude and phase angle of the electric signals. However, the waveform-based methodologies commonly perform a track of patterns and behaviors in the signals by performing a feature extraction. These features used to be statistical, entropy-based features, energy features, among others. The selection of these features is not a trivial task, and it has a very deep impact on the accuracy of the results. Therefore, to properly select the relevant features and to discard redundant information, the waveform-based methodologies implement complimentary processing for the optimized feature selection. Additionally, the use of several features results in a high number of parameters to describe a single PQD, and to obtain an accurate classification, it is necessary to implement a complex classification scheme that requires of the tuning of a high number of parameters; many times, the optimum performance is not achieved even after multiple trials. Thus, in this work, a 2D-CNN is used that performs the feature extraction and the classification in a single step, without requiring of the tuning of many parameters. The tradeoff of using this technique is that the input of the 2D-CNN is an image, and the only preprocessing that is performed is a resizing, which is a simple task. In this sense, the use of image processing is helpful for reducing the complexity of the optimal feature selection and the high number of parameters to be tuned in the classification task by using a single technique (2D-CNN) to perform all these steps.

4.3. Comparative Analysis

Observing the results shown above, it is clear that the proposed methodology has been able to adequately classify the different phenomena related to PQDs with a global classification ratio up to 99.48%, for all the six power disturbances. However, with the purpose of demonstrating the effectiveness of the proposed approach, a comparative analysis versus some previously mentioned works in the introduction section is carried out. In this sense, Table 2 summarizes the results obtained by the previous literature and also shows the conditions evaluated, as well as the used classification technique.

Table 2. Comparison of different techniques and performances.

Ref	PQD	ND Technique	Noise	Total Performance (%)
[19]	Normal, sag, swell, harmonic, fluctuation	Feature extraction/ NN	N/A	99.7% (≈79% for sag)
[20]	Normal, harmonics, interruption, notch, sag, swell, transient impulse	Cubic SVM	N/A	99.7% (≈79% for sag)
[22]	Normal, swell, swell with harmonics, harmonics with oscillatory transient	OC-SVM	Combination of PQDs	94.2%
[23]	Normal, interruption, harmonics	Auto encoder	N/A	80.0%
[24]	Normal, impulsive, interruption, oscillatory, sag, swell	2D-CNN	30 SNRdB	96.67%
Proposed	Normal, sag, swell, flicker, harmonic, transient impulse	2D-CNN with image resizing	60 SNRdB	99.4%

Results reported in [19,20] present general values with high accuracy (99.7%); however, a classification percentage around 79% has been reported when the sag disturbance appears. This situation may be explained by the fact that the behavior of a signal with a sag is very similar to one that presents a healthy signal. Another important aspect is that the signals analyzed in [19,20] are free of noise, which is an important issue that significantly affects the performance of classification when real signals are under evaluation. For the remaining works, such as in [22–24], the overall percentages show variations within the range of 80% to 96.67%, which are lower than the accuracy reached by the proposed approach. Therefore, it seems that conventional methods provide high percentages of classification accuracy, but such results are reached only because the analyzed signals are ideally perfect without noise. In contrast, methodologies where noise is considered show accuracy percentages below 97% (lower than the proposed methodology). This is because the phenomena related to PQDs are very susceptible to noise conditions, reducing the classification accuracy. Therefore, it can be emphasized that the proposed method, in comparison with approaches of previous works, shows better results of up to 99.48%, even in high noise conditions.

At this point, it is also noticeable that the proposed methodology aims to fill some of the existent gaps in the field of power quality monitoring and in the analysis of distributed generation grids with renewable sources. Beyond the high classification accuracy achieved by the proposed methodology, this approach is not affected by the window size, since the CWT performs an automatic windowing process that allows us to enhance the performance of the overall technique. In this regard, most of the proposed methodologies so far are highly dependent on the window size, and they fail in classification if the window size is not properly tuned. Also, most of the reported works so far only deal with synthetic signals where the classification of disturbances is easier than in real environments. Moreover, the analysis of distributed generation grids that contain renewable generation sources like the photovoltaic one has been scarcely reported. In this sense, the proposed work demonstrates that is able to work with signals from real environments and to perform an analysis in a power grid with PV generation, making it a tool to be used in the reliable assessment of renewable generation sources. Finally, it must be mentioned that some of the reported works so far treat the quasi-stationary disturbances and the transient disturbances separately; the methodology proposed here is able to deal with both types of disturbances

(quasi-stationary and transient) at the same time. Table 3 summarizes the strengths of the proposed approach compared with some previously reported works.

Table 3. Summary of the bullet points and strengths of the proposed methodology compared with some previously reported works.

Ref	Window Size Sensitive	Transient Disturbance Identification	Quasi-Stationary Disturbance Identification	Use Real Signals	Consider Renewable Generation Power Grids
This work	No	Yes	Yes	Yes	Yes
[19]	Yes	No	Yes	No	No
[20]	Yes	Yes	Yes	No	No
[22]	Yes	Yes	Yes	No	No
[23]	Yes	No	Yes	No	No
[24]	No	Yes	Yes	No	No

5. Conclusions

In this work, we propose a condition monitoring strategy for the detection and identification of power quality disturbances that can occur in energy generation systems that are based on renewable processes. The capability of continuous wavelet transform to highlight those representative fault-related features that are linked to the occurrence of PQD should be emphasized; hence, the obtained results demonstrate that the appearance of a PQD produces changes that can be identified through a visual analysis over the obtained spectrograms; that is, the occurrence of any of the studied disturbances may produce a specific pattern. Additionally, the processing of the spectrograms as 2D images also influences the resulting diagnosis outcome that is achieved by the proposed CNN; specifically, the selection of the optimal image size plays an important role in the training of the CNN. The proposed methodology is first validated under a synthetic set of signals where six different PQD are considered, and then, validation under a real set of signals acquired from a 30 MW photovoltaic system is also performed. According to the obtained results, the method is suitable to be implemented since it can be exported to any software containing the necessary tools for CNN development, for example PYTHON, which would facilitate its implementation in maintenance programs to detect the occurrence of disturbances in renewable-energy-based generation systems.

Also, it is worth mentioning that certain conditions contribute to generating more than one power quality disturbance at the same time, acting in a combined way, and this situation could be reflected in the collected data. For instance, the switching of several resistance load types together with the startup of some induction motors in the system can induce phenomena of sags, swells, harmonic content, and transient spikes in the power lines at the same time or combinations of them. Thus, the proposed methodology could handle these situations because of the considered deep feature-learning approach. For instance, once the signals with combined power disturbances are preprocessed in stage two, spectrogram images are created containing information of these combined disturbances. Therefore, they will be used for training the CNN structure for detection, and the SoftMax for classification. Of course, it is assumed that the signals will have different behavior in their spectrograms when an isolated disturbance is present than when combined disturbances occur. Thus, this training will provide the networks with the capability to recognize the patterns of combined disturbances to give them a category. However, these cases are detected as an area of opportunity in this work, and they will be addressed as future work. Also, hardware implementation is considered future work in order to develop a diagnostic tool for online implementations. Another point of interest is the realization of a method that allows the optimization of the area to be cut out of the image to improve the process by only containing the most relevant information of the phenomenon, depending on the sampling frequency. This can vary according to the needs of each user, allowing the automation of the entire process.

Author Contributions: Conceptualization, E.P.-A. and D.A.E.-O.; methodology, E.P.-A.; D.A.E.-O.; software, D.A.E.-O.; validation, D.A.E.-O., A.Y.J.-C. and J.J.S.-D.; formal analysis, E.P.-A.; investigation, D.A.E.-O. and J.J.S.-D.; resources, A.Y.J.-C.; data curation, E.P.-A.; writing—original draft preparation, E.P.-A.; writing—review and editing, A.Y.J.-C. and R.d.J.R.-T.; visualization, A.Y.J.-C. and R.d.J.R.-T.; supervision, R.d.J.R.-T.; project administration, R.d.J.R.-T. and J.J.S.-D.; funding acquisition, J.J.S.-D. All authors have read and agreed to the published version of the manuscript.

Funding: This project has been partially supported by the Mexican Council of Humanities Sciences and Technology (CONAHCyT) through scholarship 1078505 and by the Universidad Autonoma de Querétaro through "Fondo para el Desarrollo del Conocimiento" (FONDEC-UAQ-2022) under project number 20205007071601.

Data Availability Statement: Data are available upon request.

Conflicts of Interest: The authors declare no conflicts of interest.

References

1. United Nations (ONU). Las Energías Renovables Están a Nuestro Alrededor. Available online: https://www.un.org/es/climatechange/raising-ambition/renewable-energy#:~:text=En%202030,%20la%20electricidad%20m%C3%A1s,energ%C3%ADa%20el%C3%A9ctrica%20a%20escala%20mundial (accessed on 27 November 2023).
2. Jaen-Cuellar, A.Y.; Elvira-Ortiz, D.A.; Osornio-Rios, R.A.; Antonino-Daviu, J.A. Advances in Fault Condition Monitoring for Solar Photovoltaic and Wind Turbine Energy Generation: A Review. *Energies* **2022**, *15*, 5404. [CrossRef]
3. Lau, C.Y.; Gan, C.K.; Baharin, K.A.; Sulaima, M.F. A Review on the Impacts of Passing-Clouds on Distribution Network Connected with Solar Photovoltaic System. *IREE* **2015**, *10*, 449. [CrossRef]
4. Rahim, K.; Mohajeryami, S.; Majzoobi, A. *Effects of Photovoltaic Systems on Power Quality*; ResearchGate: Berlin, Germany, 2016.
5. Al-Hasan, A.Y.; Ghoneim, A.A. A new correlation between photovoltaic panel's efficiency and amount of sand dust accumulated on their surface. *Int. J. Sustain. Energy* **2005**, *24*, 187–197. [CrossRef]
6. Cabanillas, R.E.; Munguía, H. Dust accumulation effect on efficiency of Si photovoltaic modules. *J. Renew. Sustain. Energy* **2011**, *3*, 043114. [CrossRef]
7. Memiche, M.; Bouzian, C.; Benzahia, A.; Moussi, A. Effects of dust, soiling, aging, and weather conditions on photovoltaic system performances in a Saharan environment—Case study in Algeria. *Glob. Energy Interconnect.* **2020**, *3*, 60–67. [CrossRef]
8. Li, B.; Delpha, C.; Diallo, D.; Migan-Dubois, A. Application of Artificial Neural Networks to photovoltaic fault detection and diagnosis: A review. *Renew. Sustain. Energy Rev.* **2020**, *138*, 110512. [CrossRef]
9. Lupangu, C.; Bansal, R. A review of technical issues on the development of solar photovoltaic systems. *Renew. Sustain. Energy Rev.* **2017**, *73*, 950–965. [CrossRef]
10. *IEEE Std 1159*; IEEE Recommended Practice for Monitoring Electric Power Quality. IEEE: Piscataway, NJ, USA, 2009; Volume 2009.
11. Sharifudin, W.M.F.B.W.; Sharif, Z. Detection and Analysis of Power Quality Disturbances Using Bilinear Time-Frequency Distribution. In Proceedings of the IEEE 9th International Colloquium on Signal Processing and Its Applications, Kuala Lumpur, Malaysia, 8–10 March 2013.
12. Fuchs, E.; Trajanoska, B.; Orhouzee, S.; Renner, H. Comparison of wavelet and Fourier analysis in power quality. In Proceedings of the 2012 Electric Power Quality and Supply Reliability, Tartu, Estonia, 11–13 June 2012; pp. 1–7. [CrossRef]
13. Choi, D.-J.; Han, J.-H.; Park, S.-U.; Hong, S.-K. Comparative Study of CNN and RNN for Motor fault Diagnosis Using Deep Learning. In Proceedings of the 2020 IEEE 7th International Conference on Industrial Engineering and Applications (ICIEA), Bangkok, Thailand, 16–21 April 2020.
14. Ali, J. Power Grid Noise Analysis Using Empirical Mode Decomposition Method. Master's Thesis, University of South-Eastern Norway, Notodden, Norway, 2021.
15. Arrabal-Campos, F.M.; Montoya, F.G.; Banos, R.; Martinez-Lao, J.; Alcayde, A. Simulation of power quality disturbances through the wavelet transform. In Proceedings of the International Conference on Harmonics and Quality of Power, ICHQP, IEEE Computer Society, Ljubljana, Slovenia, 13–16 May 2018; pp. 1–5. [CrossRef]
16. Li, P.; Gao, J.; Xu, D.; Wang, C.; Yang, X. Hilbert-Huang transform with adaptive waveform matching extension and its application in power quality disturbance detection for microgrid. *J. Mod. Power Syst. Clean Energy* **2016**, *4*, 19–27. [CrossRef]
17. Srividya, T.; Sankar, M.A.M.; Devaraju, D.T. Identifying, Classifying of Power Quality Disturbances Using Short Time Fourier Transform And S-Transform. *Wkly. Sci.* **2013**, *1*, 2321–7871.
18. Singh, U.; Singh, S.N. Time–frequency–scale transform for analysis of PQ disturbances. *IET Sci. Meas. Technol.* **2017**, *11*, 305–314. [CrossRef]
19. Gonzalez-Abreu, A.D.; Saucedo-Dorantes, J.J.; Rios, R.A.O.; Romero-Troncoso, R.J.; Delgado-Prieto, M.; Morinigo-Sotelo, D. Condition monitoring approach based on dimensionality reduction techniques for detecting power quality disturbances in cogeneration systems. In Proceedings of the 2019 24th IEEE International Conference on Emerging Technologies and Factory Automation (ETFA), Zaragoza, Spain, 10–13 September 2019.

20. Aziz, S.; Khan, M.U.; Abdullah; Usman, A.; Mobeen, A. Pattern Analysis for Classification of Power Quality Disturbances. In Proceedings of the 2020 International Conference on Emerging Trends in Smart Technologies (ICETST), Karachi, Pakistan, 26–27 March 2020; pp. 1–5. [CrossRef]
21. Gonzalez-Abreu, A.-D.; Osornio-Rios, R.-A.; Jaen-Cuellar, A.-Y.; Delgado-Prieto, M.; Antonino-Daviu, J.-A.; Karlis, A. Advances in Power Quality Analysis Techniques for Electrical Machines and Drives: A Review. *Energies* **2022**, *15*, 1909. [CrossRef]
22. Gonzalez-Abreu, A.D.; Delgado-Prieto, M.; Saucedo-Dorantes, J.; Osornio-Rios, R. Novelty detection on power quality disturbances monitoring. *Renew. Energy Power Qual. J.* **2021**, *19*, 211–216. [CrossRef]
23. Zegaoui, A.; Petit, P.; Aillerie, M.; Sawicki, J.; Belarbi, A.; Krachai; Charles, J. Deep Learning based Condition Monitoring approach applied to Power Quality. *Energy Procedia* **2011**, *6*, 695–703. [CrossRef]
24. Salles, R.S.; Ribeiro, P.F. The use of deep learning and 2-D wavelet scalograms for power quality disturbances classification. *Electr. Power Syst. Res.* **2023**, *214*, 108834. [CrossRef]
25. Valtierra-Rodriguez, M.; Rivera-Guillen, J.R.; Basurto-Hurtado, J.A.; De-Santiago-Perez, J.J.; Granados-Lieberman, D.; Amezquita-Sanchez, J.P. Convolutional neural network and motor current signature analysis during the transient state for detection of broken rotor bars in induction motors. *Sensors* **2020**, *20*, 3721. [CrossRef]
26. Mukherjee, I.; Tallur, S. Light-Weight CNN Enabled Edge-Based Framework for Machine Health Diagnosis. *IEEE Access* **2021**, *9*, 84375–84386. [CrossRef]
27. Sepasi, S.; Talichet, C.; Pramanik, A.S. Power Quality in Microgrids: A Critical Review of Fundamentals, Standards, and Case Studies. *IEEE Access* **2023**, *11*, 108493–108531. [CrossRef]
28. Raja Singh, R.; Yash, S.M.; Shubham, S.C.; Indragandhi, V.; Vijayakumar, V.; Saravanan, P.; Subramaniyaswamy, V. IoT embedded cloud-based intelligent power quality monitoring system for industrial drive application. *Futur. Gener. Comput. Syst.* **2020**, *112*, 884–898. [CrossRef]
29. Ye, Z.; Shi, Y.; Gao, Z.; Wu, X. Time-Domain Hybrid Method for the Coupling Analysis of Power Line Network with Curved and Multidirectional Segments. *IEEE Trans. Electromagn. Compat.* **2022**, *65*, 216–224. [CrossRef]
30. Vahle, D.; Staudt, V. Comparison and extension of advanced frequency domain non-active power decompositions. *Electr. Power Syst. Res.* **2023**, *221*, 109448. [CrossRef]
31. Gharekhan, A.H.; Arora, S.; Panigrahi, P.K.; Pradhan, A. Distinguishing cancer and normal breast tissue autofluorescence using continuous wavelet transform. *IEEE J. Sel. Top. Quantum Electron.* **2010**, *16*, 893–899. [CrossRef]
32. Shoeb, A.; Cliord, G. Chapter 16—Wavelets; Multiscale Activity in Physiological Signals. Available online: http://www.mit.edu/~gari/teaching/6.555/LECTURE_NOTES/wavelet_lecture_notes.pdf (accessed on 5 November 2023).
33. Rioul, O.; Vetterli, M. Wavelets and signal processing. *IEEE Signal Process. Mag.* **1991**, *8*, 14–38. [CrossRef]
34. Lópes, L.F.D.M.; Lucas, C.M.; Blas, N.; Ivanova, K. Pattern Recognition with Convolutional Neural Networks: Humpback Whale Tails, Technical Report. *Preprints* **2019**, *1*, 2019020257. [CrossRef]
35. Khan, S.; Rahmani, H.; Shah, S.A.A.; Bennamoun, M. A guide to convolutional neural networks for computer vision. *Synth. Lect. Comput. Vis.* **2018**, *8*, 1–207. [CrossRef]
36. Beale, M.H.; Hagan, M.T.; Demuth, H.B. Deep Learning Toolbox™ User's Guide, MathWorks. 2020. Available online: https://www.mathworks.com/help/deeplearning/ (accessed on 25 November 2023).
37. Kim, P. *MATLAB Deep Learning*; A Press: Berkeley, CA, USA, 2017. [CrossRef]
38. Rodriguez-Guerrero, M.A.; Carranza-Lopez-Padilla, R.; Osornio-Rios, R.A.; Romero-Troncoso, R.d.J. A novel methodology for modeling waveforms for power quality disturbance analysis. *Electr. Power Syst. Res.* **2017**, *143*, 14–24. [CrossRef]